Photooxygenation of aromatic alkenes in zeolite nanocavities

Masanobu Kojima,*[a] Miyuki Nakajoh,[a] Chie Matsubara[b] and Shuichi Hashimoto[c]

[a] *Department of Bioscience and Biotechnology, Shinshu University, Kami-ina, Nagano 399-4598, Japan. E-mail: mkojima@gipmc.shinshu-u.ac.jp; Fax: +81-265-77-1629; Tel: +81-265-77-1627*

[b] *The United Graduate School of Agricultural Science, Gifu University, Gifu 501-1193, Japan*

[c] *Chemistry Department and Advanced Engineering Courses, Gunma College of Technology, Maebashi, Gunma 371-8530, Japan*

Aromatic alkenes such as styrene (**1**), 1,1-diphenylethene (**2**), and *cis*- and *trans*-stilbenes (**3**), but not triphenylethene (**4**), formed their contact charge-transfer (CCT) complexes with O_2 in solutions. In zeolite NaY, the CCT absorption band was observed only for **1** and **3**. Irradiation of alkenes **1**–**4** included in the zeolite nanocavities under O_2 produced benzaldehyde and benzophenone as the major oxygenation products. In particular, for **3** and **4**, the photooxygenation competed with a photoelectrocyclic reaction, which subsequently yielded phenanthrenes as the exclusive photoproducts under O_2 in solution. It is likely that the oxygenation products were produced through the alkene cation radicals and superoxide anion radical generated by excitation of the CCT complexes and/or photoinduced electron transfer from the excited alkenes to O_2. YAG laser (266 nm) excitation of **1** included in the zeolite cavities under vacuum produced its alkene cation radical and the trapped electron, Na_4^{3+}, both of which were quenched by O_2. On the basis of the optimum structure for the guest molecules obtained by semi-empirical molecular orbital calculations (AM1), it is suggested that the photooxygenation reaction was regulated by the electrostatic interaction between the guest molecules and alkali-metal cations in the nanocavities as well as by the strong electrostatic field which stabilized the ion radical pairs generated.

Introduction

Finding ways to regulate the photophysical and photochemical behavior of organic molecules by means of organized and constrained media has recently become an interesting and important area of research.[1–3] As one of the more promising media, zeolite nanocavities have attracted much attention in the past ten years with respect to the stabilization of the photo-excited species[4] and the enhancement of intersystem crossing for organic guest molecules by metal ions,[5] in addition to the steric effect[6–9] and the regioselectivity[10] due to the restricted spaces. We are particularly intrigued by the phenomenon, reported by Frei *et al.*,[11–15] in which an enhanced intermolecular interaction takes place between aliphatic alkenes such as 2,3-dimethylbut-2-ene and an oxygen molecule (O_2) in the alkali-metal cation-exchanged Y zeolites. Surprisingly, the contact charge-transfer (CCT) complexes formed by the inter-action exhibited extremely strong absorption spectra up to the visible wavelength region. Excitation of the CCT absorption band using a visible laser light seemed, on examination of the infrared spectra, to cause an electron transfer from the alkenes to O_2, which generated the monomer alkene cation radicals and superoxide anion radical ($O_2^{\bullet-}$), and finally formed oxygenation products through the dioxetanes and hydroperoxides.[11–15] We have been studying the photoinduced electron transfer (PET) reaction of the CCT complexes in solutions between aromatic alkenes like styrenes and O_2.[16–21] This study aims to establish whether zeolite nanocavities have potential as photochemical reaction vessels for the CCT complexes of aromatic alkenes. In a previous paper,[22] we reported that stilbenes included in alkali-metal cation-exchanged Y zeolites were photooxygenated by excitation of the CCT complexes. In this paper, we first report in detail on the differences in the spectroscopic and photochemical behavior of aromatic alkenes [styrene (**1**), 1,1-diphenylethene (**2**), stilbenes (**3**), and triphenylethene (**4**);
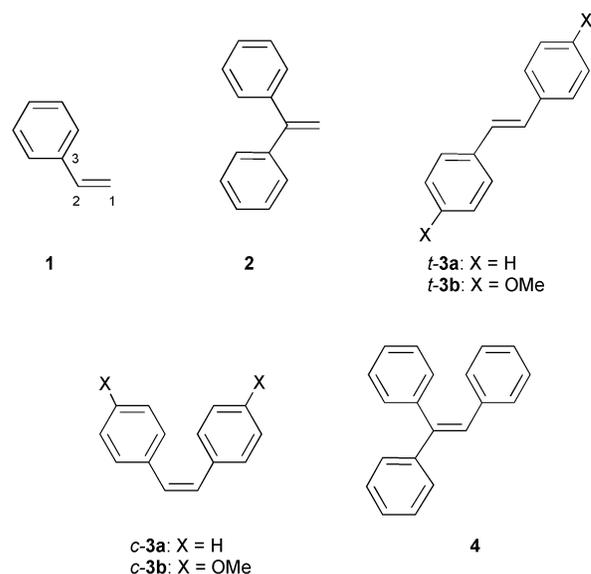
Fig. 1 Aromatic alkenes used for photooxygenation in CH_2Cl_2 and in NaY.

Fig. 1] under O_2 in zeolites and in solutions. Secondly, we suggest that the zeolite nanocavities stabilize not only the CCT complexes but also the ion radical intermediates generated by excitation of the CCT complexes and/or PET reaction between the guest molecules and O_2. This stabilization is probably due to the strong electrostatic field. Finally, it is suggested that the electrostatic interaction of metal ions with the guest molecules in the zeolite nanocavities is another important factor in regulating the photooxygenation of organic guest molecules, particularly for 1,2-diphenylethenes **3** and **4**.

Experimental

Materials

Alkenes **1** and **2** were commercial products from Wako Pure Chem. Ind., Inc. *cis-* (*c*-**3a**) and *trans*-stilbene (*t*-**3a**) and **4** were purchased from Aldrich, and *trans*-4,4′-dimethoxystilbene (*t*-**3b**) was obtained from Acros Organics. *cis*-4,4′-Dimethoxystilbene (*c*-**3b**) was prepared by irradiation of *t*-**3b** in benzene under air using a high-pressure mercury lamp (Riko UVL-400HA) and isolated by column chromatography. All the aromatic alkenes were purified by distillation under reduced pressure or recrystallized prior to use. Zeolite NaY (SiO$_2$, 67.3%; Al$_2$O$_3$, 20.3%; Na$_2$O, 12.4%; Lot No. 3001) and silica gel 60 (particle size, 0.040–0.063 mm; 230–400 mesh ASTM) were obtained from Tosoh and Merck, respectively.

3,6-Dimethoxyphenanthrene (**14b**) was prepared as follows: a 100 mL solution of 2×10^{-3} M (1 M = 1 mol dm^{-3}) *t*-**3b** in MeCN was irradiated under nitrogen using a high-pressure mercury lamp through a Pyrex filter at room temperature for 3 h. After the solvent was removed using a rotary evaporator, the products were analyzed by means of ^{1}H and ^{13}C NMR (JEOL Alpha-400 NMR spectrometer) and were identified as the corresponding isomeric dihydrophenanthrenes (**15b**). When these were oxidized by addition of a small amount of iodine to the solution, **14b** was yielded as the sole product; **14b**: MS(*m/z*) 238 (M$^+$, 100%), 223 (45%), 195 (50%), 152 (43%); ^{13}C NMR(CDCl$_3$) δ = 155.1, 131.0, 130.0, 127.1, 124.2, 116.5, 104.3, 55.6 (OMe); ^{1}H NMR(CDCl$_3$) δ = 7.96 (d, 2H), 7.79 (d, 2H), 7.56 (s, 2H), 7.24 (dd, 2H), 4.02 (s, 6H, OMe).

Measurements of oxidation potentials

The oxidation potentials (E_{ox}) of **1**–**4** were determined in MeCN by means of cyclic voltammetry using platinum as working and counter electrodes, Ag/Ag$^+$ as a reference electrode, and 0.1 M tetraethylammonium perchlorate as a supporting electrolyte.[21] For irreversible oxidation, the peak potential was taken as the oxidation potential: E_{ox}/V = 1.66 (**1**), 1.50 (**2**), 1.16 (*t*-**3a**), 1.25 (*c*-**3a**), 0.70 (*t*-**3b**), and 0.70 (*c*-**3b**) and 1.20 (**4**).[23]

Loading of alkenes into zeolite cavities

NaY (1 g) was activated at 500 °C under air for 20 h using an EYELA electric furnace TMF-1000. The activated zeolite, cooled in a desiccator, was added into a 50 mL anhydrous pentane or cyclohexane solution containing 10–40 mg of **1**–**4**. The mixture was stirred for 1 h and then kept in the dark at room temperature. After 24 h the zeolite sample was filtered, washed with anhydrous pentane or cyclohexane, and dried under vacuum. The filtrate for **1**, **2**, and **4** was analyzed, in order to confirm that the alkenes had been completely adsorbed in the zeolite cavities, using Shimadzu GC-8A and GC-14A gas chromatographs with a flame ionization detector and, respectively, either a G-100 or a G-450 capillary column (Chemicals Evaluation and Research Institute) attached. The filtrate for **3** was analyzed using a Tosoh CCP8020 high-pressure liquid chromatograph (HPLC) with a Tosoh silica-60 packed column attached. The number of guest molecules over the number of available supercages <*S*> was 0.15, 0.46, and 0.61 for **1**, 0.11 and 0.43 for **2**, 0.19 for **3**, and 0.08 for **4**.

Adsorption of 4 on silica gel

Silica gel (1 g) was activated at 500 °C under air for 5 h using an electric furnace. The activated silica gel, cooled to room temperature in a desiccator, was added into a 20 mL anhydrous pentane solution containing 10 mg of **4**. The mixture was stirred for 10 min and then kept in the dark at room temperature without a stopper in order to remove the solvent. After 10 h, the silica gel sample adsorbing **4** was dried under vacuum, as in the preparation of the zeolite samples.

Measurements of CCT absorption spectra

Change in absorption spectra caused by interaction between **1**–**4** and O$_2$ in MeCN was measured using a Shimadzu UV-2100 UV-visible double-beam spectrophotometer, as reported in the case of 1,1-diarylethenes.[21] For the zeolite samples, the spectra were measured using a Shimadzu ISR-260 integrating sphere assembly attached to the spectrophotometer and a 30 × 30 × 4 mm quartz cell. In the solution the absorption band attributed to the CCT complexes was observed using a 0.1 mm path-length quartz cell for a solution of 2×10^{-2} M **1** and a 10 cm path-length quartz cell for the solutions of 1 M **1**, 0.05 M **2**, **3a**, and *c*-**3b**, and 0.002 M *t*-**3b**; however, the CCT absorption band for **4** could not be seen using a 0.1 M solution. On the other hand, in the case of the zeolite samples, the new absorption band attributed to the CCT complexes appeared only for **1** and **3** (excluding *c*-**3a**), but not for **2** or **4**. It was confirmed that the CCT absorption band was formed reversibly by removing and introducing O$_2$.

Irradiation of alkene in solution

The alkenes dissolved in CH$_2$Cl$_2$ (0.1 M for **1**, 0.05 M for **2** and **4**, 1×10^{-3} M for **3**) were irradiated under O$_2$ and under degassed conditions in a Pyrex tube using a high-pressure mercury lamp (>290 nm; effective excitation wavelength, 313 nm). The starting alkenes and products were analyzed using GC and HPLC.

Irradiation of zeolite and silica gel samples

The zeolite and silica gel samples (200–500 mg) were irradiated in a quartz cell (30 × 30 × 4 mm) under O$_2$ and under vacuum at room temperature using 313 nm light from a high-pressure mercury lamp and 254 nm light from a low-pressure mercury lamp (Riko UVL-160LA). After irradiation the photoproducts for the zeolite samples were extracted with 50 mL of CH$_2$Cl$_2$ and 0.1–1 mL of water, filtered using a PTFE [poly(tetrafluoroethylene)] membrane filter, and analyzed by GC and HPLC. In the case of the silica gel sample, the products were extracted with 50 mL of methanol and analyzed by GC.

Molecular orbital calculation

Geometry optimization for **1**–**4** and their complexes which interacted with sodium ion (Na$^+$) was carried out using the AM1 method in MOPAC 97 installed in CSC Chem3D Ver. 4.5 for Windows.

Diffuse reflectance laser photolysis

The experimental set-up for a nanosecond diffuse reflectance laser photolysis, applicable to the detection of transient species in optically inhomogeneous and light-scattering systems, was similar to that described previously.[24] We adopted the approach reported by Wilkinson *et al.*[25] in which percentage absorption is employed to describe the transient optical absorption signal following laser excitation of the guest-doped zeolite:

$$\text{absorption} (\%)(\lambda, \tau) = 100[1 - R(\lambda, \tau)/R_0(\lambda, \tau)]$$

where R and R_0 denote the intensities of the diffuse reflected light with and without excitation, respectively. The transient absorption spectra were corrected for luminescence by subtracting a laser-only shot signal from the initial signal trace.

Results and discussion

Formation of the CCT complexes

As in the cases of 4-substituted styrenes, 1-arylcyclohexenes, and 1,1-diarylethenes,[16–21] the absorption band attributable to

the CCT complexes comprising **1** and O_2 in MeCN were observed using a 10 cm path-length cell in a 310 to 450 nm wavelength region, as can be seen in Fig. 2a. When the
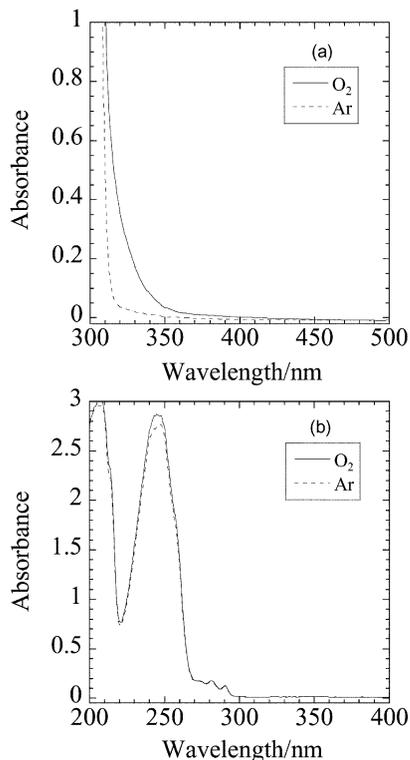
Fig. 2 Absorption spectra for CCT complexes comprising **1** and O_2 in MeCN: (a) 1 M and (b) 2×10^{-2} M.

absorption spectra for **1** were measured using a 2×10^{-2} M solution and a 0.1 mm path-length cell under O_2, the intensity of the absorption band between 230–260 nm was *ca.* 0.15 greater than that measured under argon, whereas no significant spectral change was observed in the 310 to 450 nm wavelength region, as can be seen in Fig. 2b. The increase in intensity of the absorption band was reversed by exchanging argon for O_2; therefore, this spectral change is due to the formation of the CCT complex between **1** and O_2. Because the absorption spectra for the CCT complexes were previously measured at higher concentrations, the CCT absorption band was observed only in wavelength regions longer than those attributed to the organic substrates.[26–28] The present results obtained for **1** in a lower concentration indicate that the CCT absorption band may overlap with that of the substrate itself, as can be seen in UV absorption spectra for **1** and aromatic hydrocarbons measured in the cryogenic oxygen matrix.[29] The CCT absorption bands were also observed for **2** and **3** in MeCN in the 310–360 and 375–500 nm regions, respectively.

In NaY the new absorption was observed under O_2 only for **1** and **3** (though not for *c*-**3a**), as shown in Fig. 3. For **1** the intensity of the absorption at around 250 nm increased with increase in the partial pressure of O_2, as can be seen in Fig. 3a; in addition, it was found that this spectral change could be reversed by changing the partial pressure. Thus, we attributed the new absorption to the formation of the CCT complex. The CCT band observed was similar to that of **1** in a lower concentration in MeCN (Fig. 2b), although the weak absorption band could also be seen in a longer wavelength region in the case of *t*-**3a** and *t*-**3b**.[22] For the zeolite samples, a CCT absorption band overlapping with that of the guest molecules was clearly observed by means of diffuse reflectance spectra, similar to the case of 4-methoxystyrene and methoxybenzene adsorbed in NaY.[30] However, no significant enhancement in the formation of the CCT complexes was seen in the visible wavelength region
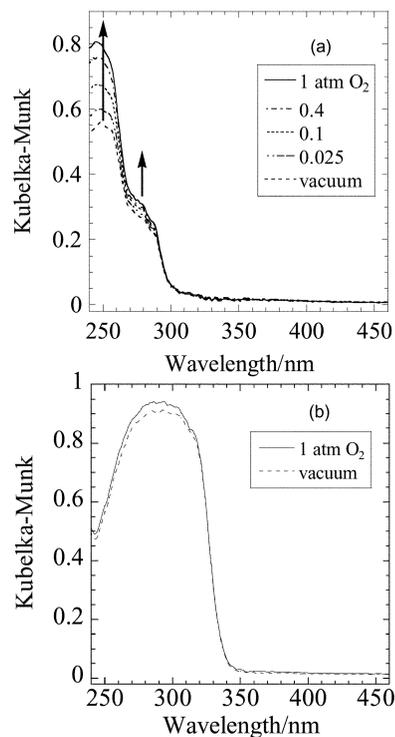
Fig. 3 Diffuse reflectance absorption spectra for **1** (a: $\langle S \rangle = 0.15$) and *t*-**3a** (b: $\langle S \rangle = 0.19$) in NaY observed under O_2 (0.025–1 atm).

for **1** and **3**, in contrast to the case of aliphatic alkenes reported by Frei *et al.*[11–15] In the case of **2** and *c*-**3a**, which formed the CCT complexes with O_2 in MeCN, no new absorption band attributable to the CCT complexes was observed. This indicates that zeolite nanocavities do not necessarily favor the formation of the CCT complexes for aromatic alkenes. As discussed later, this is probably due to the electrostatic interaction of the alkenes with the metal cations in the cavities.

On the basis of the oxidation potentials measured by cyclic voltammetry, **4** ($E_{ox}/V = 1.20$ *vs.* Ag/Ag^+) is more electron-donating than **1** and **2** (1.67 and 1.50 V). However, the CCT complex comprising **4** and O_2 was not formed either in MeCN or in NaY. Therefore for the formation of the CCT complex, both the formation of structures with less steric hindrance as well as the property of donating electrons are important. As in the reaction of $^1O_2$ with a carbon–carbon double bond, the CCT complex would require a strict geometry of oxygen with the π systems.[31]

Photochemical reaction of aromatic alkenes under O_2 in solution and in zeolite

(a) For phenylethene (1). Irradiation of **1** in CH_2Cl_2 under argon using 313 nm light yielded [2 + 2] and [2 + 4] cyclodimers **9** as the dominant products (distribution of product, 95%) as found by Brown (Entry 1 in Table 1).[32] However, under O_2, production of benzaldehyde (**5a**, 44%) and styrene oxide (**7**, 20%) competed with the dimer formation (30%), as shown in eqn. (1) and Entry 2, Table 1. When a zeolite sample of **1** ($\langle S \rangle = 0.46$) adsorbed in NaY was irradiated under vacuum using 313 nm light, cyclodimers **9** were the dominant products (84%, Entry 3) as in the photoreaction in CH_2Cl_2 under argon. Formation of 14% **5a** is probably due to a small amount of air leaking in during irradiation. It is worth noting that formation of **9** was entirely suppressed when the zeolite sample was irradiated under O_2 and that **5a** was formed in a yield of 75% (Entry 4). Phenylacetaldehyde (**6**) was produced only in NaY as a photooxygenation product; however, it was confirmed that **7** was unstable in the cavities and readily gave **6** in the dark. Although photodimerization under vacuum in NaY was seen

Table 1 Photooxygenation of **1** in CH$_2$Cl$_2$ and in NaY

Entry	Conditions	Conversion (%)	Total yield[a].(%)	Distribution of products[b] (%)				
				5a	**6**	**7**	**8**	**9**
1	Ar/CH$_2$Cl$_2$/>290 nm [c]	11	41	2	—	3	—	95
2	O$_2$/CH$_2$Cl$_2$/>290 nm [c]	21	43	44	—	20	6	30
3	Vacuum/NaY/>290 nm [cd]	7	9	14	—	—	2	84
4	O$_2$/NaY/>290 nm [cd]	20	62	75	22	—	3	Trace
5	Vacuum/NaY/254 nm [de]	5	30	7	—	—	—	93
6	O$_2$/NaY/254 nm [de]	10	29	73	17	—	Trace	10

[a] Total yield of products based on the amount of **1** consumed. [b] Yield (%) based on the initial amount of **1** = conversion × (total yield/100) × (distribution of products/100). [c] Irradiated through a Pyrex filter using a high-pressure mercury lamp (effective excitation wavelength, 313 nm) for 2 h. [d] <S> = 0.46. [e] Irradiated through a quartz filter using a low-pressure mercury lamp for 2 h.

Table 2 Photooxygenation of **2** in CH$_2$Cl$_2$ and in NaY

Entry	Conditions[a]	Conversion (%)	Total yield[b] (%)	Distribution of products[c] (%)			
				10	**11**	**12**	**13**
1	Degassed/CH$_2$Cl$_2$	3	—	—	—	—	—
2	O$_2$/CH$_2$Cl$_2$	35	43	51	—	21	28
3	Vacuum/NaY[d]	3	—	—	—	—	—
4	O$_2$/NaY[d]	53	50	74	20	—	6

[a] Irradiated through a Pyrex filter using a high-pressure mercury lamp (>290 nm; effective excitation wavelength, 313 nm) for 5 h. [b] Total yield of products based on the amount of **2** consumed. [c] Yield (%) based on the initial amount of **2** = conversion × (total yield/100) × (distribution of products/100). [d] <S> = 0.11.

to proceed exclusively, the efficiency was lower than that in CH$_2$Cl$_2$ (see the conversion and total yield in Entries 1 and 3). This may be due to the small number of <S> and also to the fact that the diffusion rate of guest molecules between the cavities was slower than that in solution.[33] When the zeolite sample was irradiated using 254 nm light (Entries 5 and 6), the product distribution was similar to that obtained using 313 nm light, although the CCT absorption maximum was observed around 250 nm, as can be seen in Fig. 3a.

$$1 \xrightarrow[\text{NaY/O}_2]{h\nu} \underset{\mathbf{5a}}{\text{PhCHO}} + \underset{\mathbf{6}}{\text{PhCH}_2\text{CHO}} + \underset{\mathbf{7}}{\overset{\text{Ph}}{\bigtriangledown}\text{O}} + \underset{\mathbf{8}}{\text{PhCOMe}} + \underset{\mathbf{9}}{\text{Dimers}} \quad (1)$$
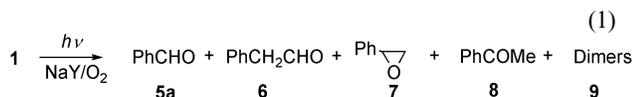
(b) For 1,1-diphenylethene (2). We have already reported on a study of the photochemical reactions of the CCT complexes between 1,1-diarylethenes and O$_2$, in which 3,3,6,6-tetraaryl-1,2-dioxanes and benzophenones were the major products through the PET reaction of the complexes.[20,21] With respect to **2**, benzophenone (**10**) was analyzed in the present study together with other photooxygenation products in order to re-examine the reaction in detail, as shown in Table 2 and eqn. (2). Under degassed conditions in CH$_2$Cl$_2$ and under vacuum in NaY (Entries 1 and 3), no significant photoreaction occurred using 313 nm light. In contrast, diphenylmethane (**11**), 1,1-diphenylethanol (**12**), and diphenylacetaldehyde (**13**) together with **10** were found to be the main oxygenation products. Both in CH$_2$Cl$_2$ and in NaY, **10** was obtained as the major product (51 and 74%, respectively); however, it should be noted that, on the basis of the conversion and distribution of the products (Entries 2 and 4), the reactivity of **2** and product selectivity to give **10** was *ca.* 20% greater in NaY than in CH$_2$Cl$_2$. Although **11** was yielded as a specific product in NaY, suppressing the formation of **12** and **13**, it was found that **11** was a secondary product from **13**. Therefore, the photodecomposition of **13** to **11** seems to occur more readily in NaY than in solution. Although an enhancement of the fragmentation might be an interesting characteristic of the zeolite cavities, we have not pursued this area because it was not a photoreaction specific to the cavities. The production of **12**

may occur through an autooxidation mechanism, as reported for 2-phenylpropene and 2-methyl-1,1-diphenylpropene.[34] Accordingly, NaY might be an unfavorable environment for autooxidation, as in the case of **1**, due both to the small number of <S> and to the fact that the diffusion rate of guest molecules between the cavities is slower than that in solution.

$$2 \xrightarrow[\text{NaY/O}_2]{h\nu} \underset{\mathbf{10}}{\text{Ph}_2\text{CO}} + \underset{\mathbf{11}}{\text{Ph}_2\text{CH}_2} + \underset{\mathbf{12}}{\text{Ph}_2\text{C(OH)CH}_3} + \underset{\mathbf{13}}{\text{Ph}_2\text{CHCHO}} \quad (2)$$
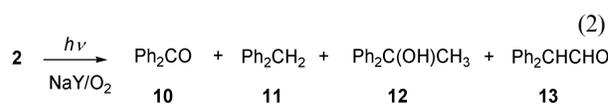
(c) For 1,2-diphenylethene (3). When *c*- and *t*-**3a** were irradiated using 313 nm light under O$_2$ in CH$_2$Cl$_2$, PhH, MeCN, and cyclohexane, phenanthrene (**14a**) was yielded quantitatively in all the solvents as the final photostable product [eqn. (3)]. As mentioned already, the CCT complexes for **3a** are formed in solutions; however, the result clearly shows that the photochemical reaction through excitation of the complexes does not occur at all in solutions. This is probably because a photoelectrocyclic reaction in solutions occurs much faster than photooxygenation.

$$(3)$$
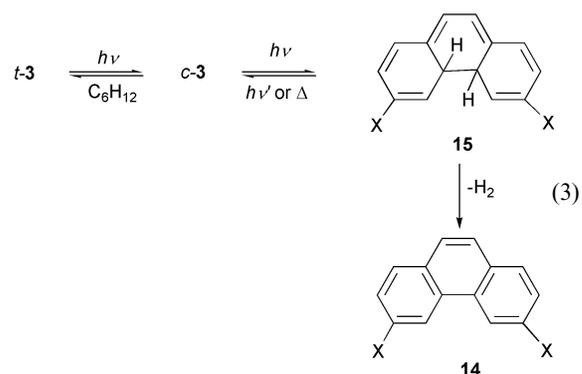
For *c*- and *t*-**3b**, on the other hand, irradiation of the solutions under O$_2$ gave a different product distribution; namely, no dimethoxyphenanthrene **14b** was produced, and

Table 3 Product distribution yielded on irradiation of **3** in NaY under O_2

Entry	**3**	Conditions[a][b]	Total yield[c] (%)	Distribution of products (%)			
				c-**3**	t-**3**	**14**	**5**
1	c-**3a**	NaY/C_6H_{12}[d]	82	83	17	Trace	—
2	c-**3a**	NaY	24	74	11	5	10
3	t-**3a**	NaY/C_6H_{12}[d]	86	24	76	Trace	—
4	t-**3a**	NaY	43	56	30	7	7
5	c-**3b**	NaY	47	82	12	—	6
6	t-**3b**	NaY	46	46	38	—	16

[a] Irradiated through a Pyrex filter using a high-pressure mercury lamp (>290 nm; effective excitation wavelength, 313 nm) for 4 h. [b] <S> = 0.19. [c] Total yield of starting **3** and products. [d] Irradiated while being stirred in cyclohexane.

Table 4 Photooxygenation of **4** in CH_2Cl_2 and in NaY and on silica gel

Entry	Conditions[a]	Conversion (%)	Total yield[b] (%)	Distribution of products[c] (%)		
				5a	**10**	**17**
1	Degassed/CH_2Cl_2	0	—	—	—	—
2	O_2/CH_2Cl_2	38	90	5	12	83
3	Vacuum/NaY[d]	6	9	—	—	100
4	O_2/NaY[d]	49	24	33	29	38
5	Vacuum/silica gel	21	6	—	—	100
6	O_2/silica gel	83	60	3	5	92

[a] Irradiated through a Pyrex filter using a high-pressure mercury lamp (>290 nm; effective excitation wavelength, 313 nm) for 5 h. [b] Total yield of products based on the amount of **4** consumed. [c] Yield (%) based on the initial amount of **4** = conversion × (total yield/100) × (distribution of products/100). [d] <S> = 0.08.

instead, dimethoxydihydrophenanthrene isomers **15b** were formed together with 4-methoxybenzaldehyde (**5b**). It has been reported that some dihydrophenanthrenes formed from the corresponding *cis*-stilbenes are stable even under O_2; therefore, the addition of oxidants stronger than O_2 is useful in the preparation of phenanthrenes.[35,36] In fact, when 2×10^{-3} M *t*-**3b** was irradiated in MeCN under nitrogen using a high-pressure mercury lamp for 3 h, isomeric **15b** was observed using NMR. Addition of a small amount of iodine into the isomers produced **14b** as the sole product. Therefore, it was found that **15b** was particularly stable under O_2 and oxidized very slowly to **14b**.

When NaY including **3a** was irradiated while being stirred in cyclohexane under O_2 using 313 nm light, *cis–trans* isomerization was the dominant reaction and formation of **14a** was almost entirely suppressed, as shown in Entries 1 and 3, Table 3. This is probably because photooxygenation of the solvent competed with the photooxygenation of **3a**, as found by Frei *et al*.[14] In contrast, when the zeolite sample dried under vacuum was irradiated without the solvent under similar conditions, a significant amount of **5a** (10% for *c*-**3a** and 7% for *t*-**3a**, Entries 2 and 4) was produced, together with *c*- and *t*-**3a** (*ca.* 85%) and **14a** (*ca.* 6%). For **3b**, irradiation of the dried NaY sample with 313 nm light caused *cis–trans* isomerization and the production of **5b** as in the photoreaction in solutions (Entries 5 and 6). However, no **14b** or **15b** was detected by HPLC. These results suggest that zeolite cavities are an extremely unfavorable environment for the photoelectrocyclic reaction of stilbenes.

(d) For triphenylethene (4). As can be seen in Table 4, under degassed conditions, no photoreaction of **4** occurred in CH_2Cl_2 (Entry 1). Under O_2, on the other hand, **4** underwent an exclusively electrocyclic reaction to give 9-phenylphenanthrene (**17**, 83%) in CH_2Cl_2, as in the case of **3a** (Entry 2). It is noteworthy that photooxygenation of **4** in NaY to yield **5a** and **10** (33 and 29%, respectively) competed with the formation of **17** (38%, Entry 4), whereas a comparatively small amount of **17** was formed under vacuum (conversion, 6%; total yield 9%;

Entry 3). This might be either because air leaked in during irradiation or because the dihydrophenanthrene produced from **4** was stabilized in the cavities and reacted with O_2 to give **17** when the reaction cell was opened. Therefore, as indicated above, it seems likely that the zeolite cavities have a suppression effect on the electrocyclic reaction of stilbene derivatives. In order to further confirm this effect, photooxygenation of **4** adsorbed on the silica gel surface was carried out, as shown in Entries 5 and 6. Under degassed conditions, as in NaY, a small amount of **17** (yield, 6%) was produced; in contrast, **17** (yield, 55%) was the dominant product under O_2, formed on the surface through a photoelectrocyclic reaction. Accordingly, there can be no doubt that the photoelectrocyclic reaction became remarkably slow in the zeolite nanocavities. We suggest that this is due to the electrostatic interaction of the alkenes with Na^+ in the cavities, as discussed below on the basis of semiempirical molecular orbital calculations.[37–39]

$$4 \xrightarrow[\text{NaY/}O_2]{h\nu} \mathbf{5a} + \mathbf{10} + \mathbf{17} \qquad (4)$$
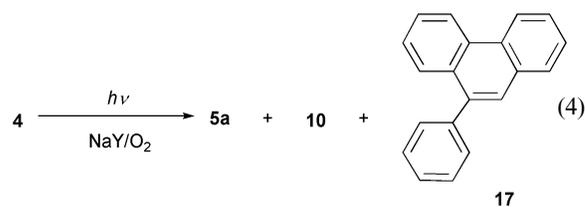
Transient absorption spectra observed on 266 nm laser excitation of 1 in NaY

Although photooxygenation of organic substrates by excitation of the CCT band has been widely studied in solution, few transient absorption spectra for reactive intermediates generated in the reaction have been reported. For example, Tsubomura *et al*. studied flash photolysis of aniline derivatives in solutions in oxygenated and deoxygenated conditions.[40] The transient spectra, caused by the cation radical of the anilines, were observed in deoxygenated ethanol, but not in oxygenated ethanol. In addition, Ogilby *et al*. observed singlet oxygen ($^1O_2$) at 1270 nm in a time-resolved experiment subsequent to pulsed

UV laser photolysis of the CCT absorption bands of organic molecules with O_2.[41,42] In contrast with the studies of reactions in solution, there has been no investigation of transient species generated by photolysis of the CCT complexes between organic guest molecules and O_2 formed in zeolites. As shown in Fig. 4a,
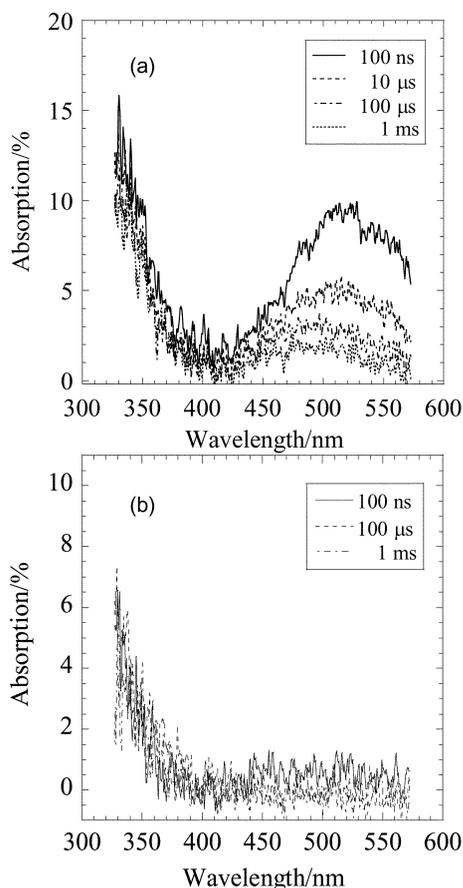
Fig. 4 Transient absorption spectra observed on 266 nm laser excitation of **1** (<*S*> = 0.46 and 0.61) in NaY under vacuum (a) and at 0.2 atm O_2 (b).

we measured the transient absorption spectra observed by excitation of **1** included in NaY using a Nd:YAG-laser photolysis system (266 nm; laser power, 2 mJ) under vacuum. The transient absorption bands appearing at around 330 and 520 nm were attributable to a cation radical of **1** ($1^{•+}$)[43] and the trapped electron (Na_4^{3+})[24,44,45] according to the literature. We could not determine if this ionization process was mono-photonic or biphotonic because, due to the limitation of our system, the range through which the power of the laser could be adjusted was too narrow. However, on the basis of the ionization potential of **1** (8.50 eV)[46] and the energy of 266 nm light (4.66 eV), it is likely that this ionization occurred through a biphotonic process even though the zeolite cavities lowered the ionization potential to some extent through the effect of the strong electrostatic field.[47] At 0.2 atm O_2 both absorption intensity of $1^{•+}$ and Na_4^{3+} sharply decreased, as can be seen in Fig. 4b. This indicates that Na_4^{3+} is rapidly oxidized by O_2 to yield $O_2^{•-}$, while $1^{•+}$ reacts with O_2 or $O_2^{•-}$. This result suggests that the reaction of $1^{•+}$ with O_2 or $O_2^{•-}$ is an important process in the production of the oxygenation products of **1** in the cavities.

Electrostatic interaction of Na^+ with alkenes

Using the AM1 Method, the optimum structure of **1–4** and their complexes with Na^+ were calculated as in the case of 4-methoxystyrene and azobenzene.[30,48] In the case of **1**, Na^+ interacts with π-electrons on C2 and C3 carbons (complex **I** in
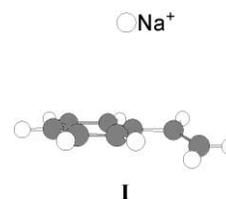
Fig. 5 Optimum structure of **1**/Na^+ complex (**I**) calculated using AM1 Method.

Fig. 5; see Fig. 1 for the carbon numbers). This interaction site is similar to that for *t*-**3a** reported previously.[48] For **2** there are several interaction sites, as shown in Fig. 6 (complexes **II**, **III**, and **IV**); however, on the basis of the heat of formation (ΔH_f): 358 kJ mol^{-1} for **II**, 362 kJ mol^{-1} for **III**, and 380 kJ mol^{-1} for **IV**, the most favorable interaction with Na^+ can be seen to occur between the two benzene rings of **2**. When *c*-**3a** interacts electrostatically with Na^+, the more stable interaction occurs between the two benzene rings (complex **V**, ΔH_f = 348 kJ mol^{-1}) rather than on the ethylene bond (complex **VI**, ΔH_f = 351 kJ mol^{-1}), as shown in Fig. 7. However, given the small difference in ΔH_f between **V** and **VI**, these complexes may coexist in the cavities. Similar interaction seems to occur for **4**, as can be seen in Fig. 8 (complexes **VII** and **VIII**; ΔH_f = 462 kJ mol^{-1} and 460 kJ mol^{-1}, respectively). The complexes **VII** and **VIII** are more stable than the other complex **IX** (ΔH_f = 465 kJ mol^{-1}), in which Na^+ interacts with the π-electrons mainly on the ethylene bond. The differences in ΔH_f among the three complexes are relatively small (2~5 kJ mol^{-1}); therefore, these complexes would coexist in the zeolite cavities, as in the case of **2** and **3**. As noted in the discussion of the distribution of photooxygenation products for **3** and **4**, the rate of the photo-electrocyclic reaction giving **14** and **17** is slower in the zeolite cavities than in solutions. This is probably because of the interaction of Na^+ with the π-electrons of the two benzene rings attached to the ethylene bond (see complexes **V** and **VII**), as found in the case of naphthalene[49] and *cis*-1,2-diphenylcyclopropane,[39] which suppresses the electrocyclic reaction.

Photooxygenation in zeolite nanocavities

(a) Role of CCT complex. It is surprising to discover that zeolite cavities have the effect of stabilizing the CCT complexes comprising aliphatic alkenes and O_2.[11–15] In the case of the aromatic alkenes employed in this study, however, the formation of the CCT complexes is not necessarily accelerated in NaY; rather, suppression of the formation was seen for **2** and *c*-**3a**. Therefore, the photooxygenation of **1–4** observed is understood to proceed through excitation of the CCT complexes and/or PET reaction between excited **1–4** and O_2 to generate the alkene cation radicals and $O_2^{•-}$.

It is expected that the strong electrostatic field in the zeolite cavities stabilizes the CCT complexes, as suggested in previous studies using aliphatic alkenes and alkyl substituted benzenes.[11–15,50,51] However, in the case of the aromatic alkenes, the formation of the CCT complexes are not essential in initiating photooxygenation. For **2** and **4**, photooxygenation in NaY occurred even though the CCT complexes were not observed. Therefore, the acceleration of the oxygenation observed particularly for **1** and **2** seems to be due to stabilization, by the electrostatic field, of the alkene cation radicals and $O_2^{•-}$, generated as the reactive intermediates.

(b) Mechanism. We propose Scheme 1 and 2 as the mechanism for the photooxygenation of **1–4** in NaY. As shown in Scheme 1, excitation of the CCT complexes and/or PET reaction of alkenes **1** and **2** with O_2 would generate the alkene cation radicals and $O_2^{•-}$, followed by cycloaddition between
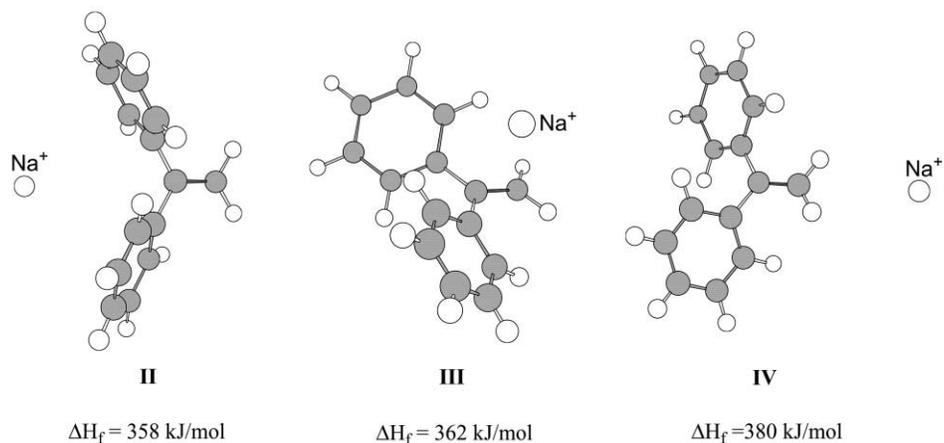
Fig. 6 Optimum structure of **2**/Na$^+$ complexes (**II**, **III**, and **IV**) obtained by AM1 calculation.

II

$\Delta H_f = 358$ kJ/mol

III

$\Delta H_f = 362$ kJ/mol

IV

$\Delta H_f = 380$ kJ/mol
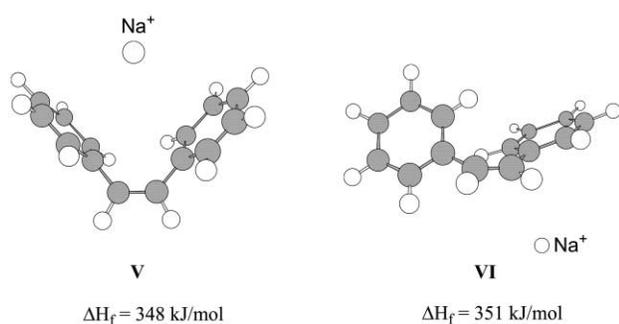
Fig. 7 Optimum structure of *c*-**3a**/Na$^+$ complexes (**V** and **VI**).

V

$\Delta H_f = 348$ kJ/mol

VI

$\Delta H_f = 351$ kJ/mol

the ion radical pair to give dioxetanes **16**, which readily decomposes to **5** and **10**, or by the reaction of the alkene cation radicals with O$_2$. The route for the production of the

corresponding epoxide is not understood at this stage. However, the instability of the epoxide in the zeolite cavities is due to the existence of Brønsted acid sites.[52,53] For 1,2-diphenylethenes **3** and **4**, the electrostatic interaction of Na$^+$ with the two benzene rings, as shown in Scheme 2, makes an electrocyclic reaction slower than in solutions, due to steric hindrance on the bond formation. Therefore, it is probable that photooxygenation through excitation of the CCT complex and/or PET reaction between the alkenes and O$_2$ competes with the electrocyclic reaction. Finally, it is possible that ^{1}O$_2$ is generated by excitation of the CCT complex and by sensitization of O$_2$ by the excited alkenes. However, it is known that aromatic alkenes are less reactive with ^{1}O$_2$ than aliphatic alkenes[54] and also that ^{1}O$_2$ reaction gives oxygenation products different from those yielded through PET;[55–57] accordingly we conclude that ^{1}O$_2$ is not the reactive oxygen species in the present reaction.

VII

$\Delta H_f = 462$ kJ/mol

VIII

$\Delta H_f = 460$ kJ/mol

IX

$\Delta H_f = 465$ kJ/mol
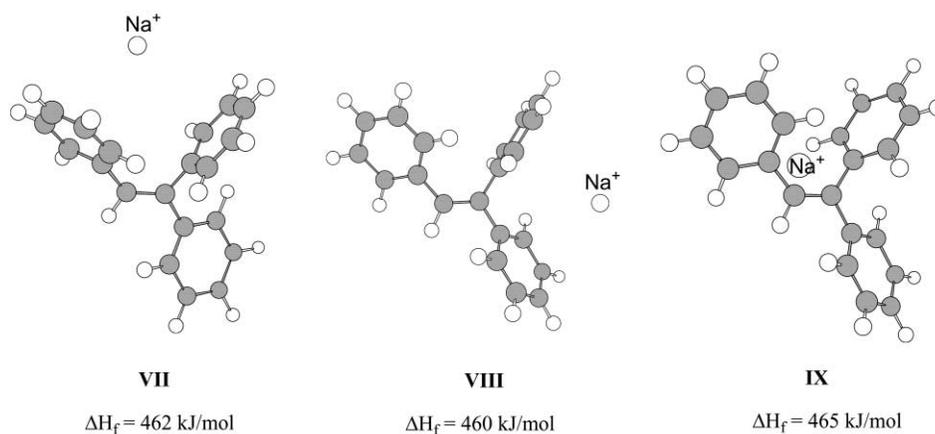
Fig. 8 Optimum structure of **4**/Na$^+$ complexes (**VII**, **VIII**, and **IX**).
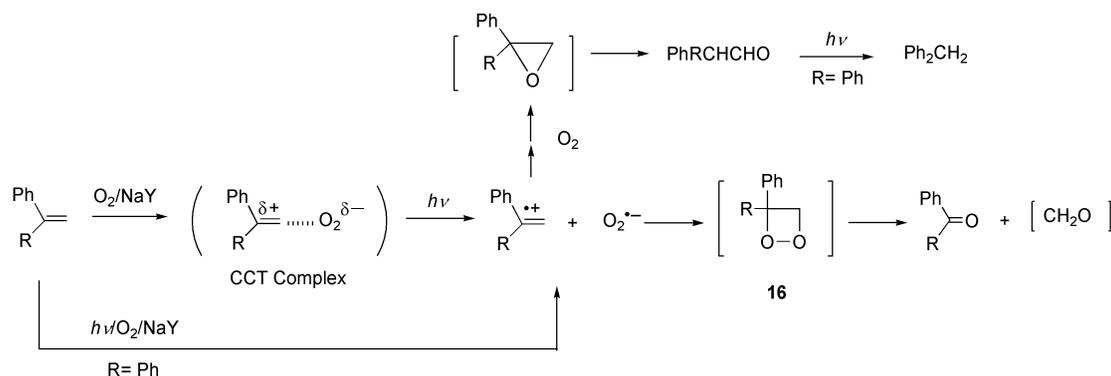
Scheme 1 Mechanism for photooxygenation of **1** and **2** in NaY: R = H and Ph.
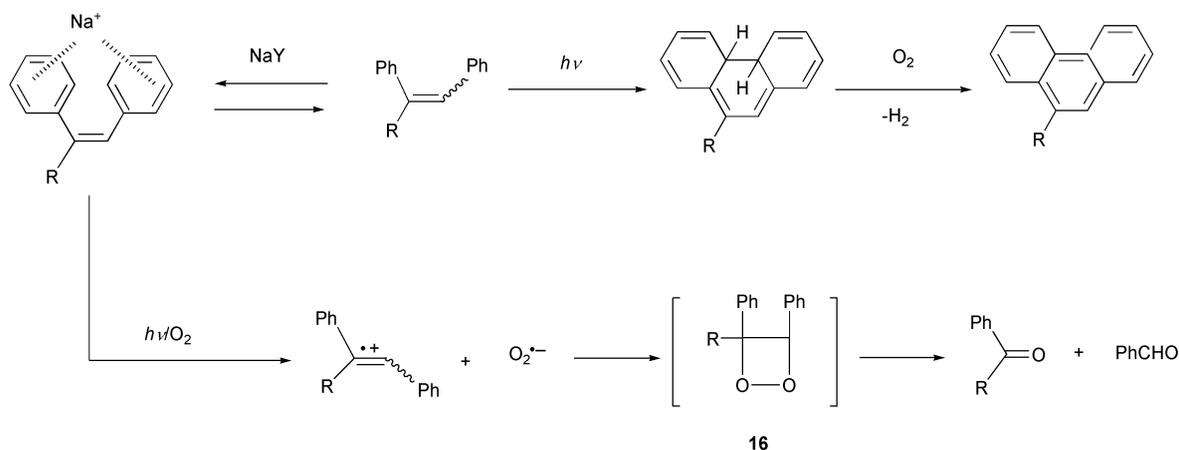
Scheme 2 Mechanism for photooxygenation of **3a** and **4** in NaY: R = H and Ph.

References

1 V. Ramamurthy, *Photochemistry in Organized and Constrained Media*, VCH, New York, 1991.
2 M. Anpo, *Surface Photochemistry*, Wiley, Chichester, 1996, vol. 1.
3 M. Kojima, *Photochemistry*, 2000, **31**, 173.
4 V. Ramamurthy, *Chimia*, 1992, **46**, 359.
5 V. Ramamurthy, J. V. Caspar, D. F. Eaton, E. W. Kuo and D. R. Corbin, *J. Am. Chem. Soc.*, 1992, **114**, 3882.
6 V. Ramamurthy, D. R. Corbin, N. J. Turro, Z. Zhang and M. A. Garcia-Garibay, *J. Org. Chem.*, 1991, **56**, 255.
7 G. Lem, N. A. Kaprinidis, D. I. Schuster, N. D. Ghatlia and N. J. Turro, *J. Am. Chem. Soc.*, 1993, **115**, 7009.
8 N. J. Turro, N. Han, X. Lei, J. R. Fehlner and L. Abrams, *J. Am. Chem. Soc.*, 1995, **117**, 4881.
9 F. Gessner, A. Olea, J. H. Lobaugh, L. J. Johnston and J. C. Scaiano, *J. Org. Chem.*, 1989, **54**, 259.
10 M. V. Baldoví, A. Corma, H. García and V. Martí, *Tetrahedron Lett.*, 1994, **35**, 9447.
11 F. Blatter and H. Frei, *J. Am. Chem. Soc.*, 1993, **115**, 7501.
12 F. Blatter and H. Frei, *J. Am. Chem. Soc.*, 1994, **116**, 1812.
13 F. Blatter, F. Moreau and H. Frei, *J. Phys. Chem.*, 1994, **98**, 13403.
14 H. Sun, F. Blatter and H. Frei, *J. Am. Chem. Soc.*, 1996, **118**, 6873.
15 S. Vasenkov and H. Frei, *J. Phys. Chem. B*, 1997, **101**, 4539.
16 M. Kojima, H. Sakuragi and K. Tokumaru, *Tetrahedron Lett.*, 1981, **22**, 2889.
17 M. Kojima, H. Sakuragi and K. Tokumaru, *Bull. Chem. Soc. Jpn.*, 1987, **60**, 3331.
18 M. Kojima, H. Sakuragi and K. Tokumaru, *Bull. Chem. Soc. Jpn.*, 1989, **62**, 3863.
19 K. Onodera, G. Furusawa, M. Kojima, M. Tsuchiya, S. Aihara, R. Akaba, H. Sakuragi and K. Tokumaru, *Tetrahedron*, 1985, **41**, 2215.
20 M. Kojima, A. Ishida and S. Takamuku, *Chem. Lett.*, 1993, 979.
21 M. Kojima, A. Ishida and S. Takamuku, *Bull. Chem. Soc. Jpn.*, 1998, **71**, 2211.
22 H. Takeya, Y. Kuriyama and M. Kojima, *Tetrahedron Lett.*, 1998, **39**, 5967.
23 F. D. Lewis, A. M. Bedell, R. E. Dykstra, J. E. Elbert, I. R. Gould and S. Farid, *J. Am. Chem. Soc.*, 1990, **112**, 8055.
24 S. Hashimoto, T. Mutoh, H. Fukumura and H. Masuhara, *J. Chem. Soc., Faraday Trans.*, 1996, **92**, 3653.
25 F. Wilkinson, *J. Chem. Soc., Faraday Trans. 2*, 1986, **82**, 2073.
26 D. F. Evans, *J. Chem. Soc.*, 1953, 345.
27 D. F. Evans, *J. Chem. Soc.*, 1956, 1351.
28 H. Tsubomura and R. S. Mulliken, *J. Am. Chem. Soc.*, 1960, **82**, 5966.
29 S. Hashimoto and H. Akimoto, *J. Phys. Chem.*, 1989, **93**, 571.
30 C. Matsubara and M. Kojima, *Res. Chem. Intermed.*, 2001, **27**, 975.
31 N. J. Turro, *Tetrahedron*, 1985, **41**, 2089.
32 W. B. Brown, *J. Am. Chem. Soc.*, 1968, **90**, 1916.
33 A. V. Barzkin and S. Hashimoto, *J. Chem. Phys.*, 2000, **113**, 2841.
34 T. Kanno, M. Hisaoka, H. Sakuragi and K. Tokumaru, *Bull. Chem. Soc. Jpn.*, 1981, **54**, 2330.
35 J. Bendig, M. Beyermann and D. Kreysig, *Tetrahedron Lett.*, 1977, 3659.
36 A. Buquet, A. Couture and A. Lablache-Combier, *J. Org. Chem.*, 1979, **44**, 2300.
37 Y. Kuriyama, H. Takeya, S. Oishi and M. Kojima, *Chem. Lett.*, 1998, 843.
38 K. Pitchumani and V. Ramamurthy, *Tetrahedron Lett.*, 1996, **37**, 5297.
39 P. Lakshminarasimhan, R. B. Sunoj, J. Chandrasekhar and V. Ramamurthy, *J. Am. Chem. Soc.*, 2000, **122**, 4815.
40 H. Hori, H. Itoi and H. Tsubomura, *Bull. Chem. Soc. Jpn.*, 1970, **43**, 3765.
41 R. D. Scurlock and P. R. Ogilby, *J. Am. Chem. Soc.*, 1988, **110**, 640.
42 R. D. Scurlock and P. R. Ogilby, *J. Phys. Chem.*, 1989, **93**, 5493.
43 T. Shida, *Electronic Absorption Spectra of Radical Ions*, Elsevier, Amsterdam, 1988.
44 K. K. Iu and J. K. Thomas, *J. Phys. Chem.*, 1991, **95**, 506.
45 K. K. Iu, X. Liu and J. K. Thomas, *J. Photochem. Photobiol. A*, 1994, **79**, 103.
46 S. L. Murov, I. Carmichael and G. L. Hug, *Handbook of Photochemistry*, Marcel Dekker, New York, 1993.
47 V. Ramamurthy, D. F. Eaton and J. V. Casper, *Acc. Chem. Res.*, 1992, **25**, 299.
48 M. Kojima, T. Takagi and T. Goshima, *Mol. Cryst. Liq. Cryst.*, 2000, **344**, 179.
49 K. J. Thomas, R. B. Sunoj, J. Chandrasekhar and V. Ramamurthy, *Langmuir*, 2000, **16**, 4912.
50 Y. Xiang, S. C. Larsen and V. H. Grassian, *J. Am. Chem. Soc.*, 1999, **121**, 5063.
51 A. G. Panov, R. G. Larsen, N. I. Totah, S. C. Larsen and V. H. Grassian, *J. Phys. Chem. B*, 2000, **104**, 5706.
52 M. Kojima, A. Odaka, T. Nakajima and Y. Kuriyama, *Chem. Lett.*, 1999, 675.
53 K. J. Thomas and V. Ramamurthy, *Langmuir*, 1998, **14**, 6687.
54 P. Schaap and K. A. Zalkika, in *Singlet Oxygen*, ed. H. H. Wasserman and R. W. Murray, Academic Press, New York, 1979, p. 173.
55 X. Li and V. Ramamurthy, *Tetrahedron Lett.*, 1996, **37**, 5235.
56 C.-H. Tung and H. Wang, *Photogra. Sci. Photochem.*, 1997, **15**, 289.
57 C.-H. Tung, H. Wang and Y.-M. Ying, *J. Am. Chem. Soc.*, 1998, **120**, 5179.